Remote pacemaker control of chimera states in multilayer networks of neurons

Giulia Ruzzene*
Department of Information and Communication Technologies, Universitat Pompeu Fabra, Carrer Roc Boronat 138, 08018 Barcelona, Catalonia, Spain

Iryna Omelchenko, Jakub Sawicki, Anna Zakharova, and Eckehard Schöll
Institut für Theoretische Physik, Technische Universität Berlin, Hardenbergstrasse 36, 10623 Berlin, Germany

Ralph G. Andrzejak
Department of Information and Communication Technologies, Universitat Pompeu Fabra, Carrer Roc Boronat 138, 08018 Barcelona, Catalonia, Spain

(Received 16 June 2020; revised 7 September 2020; accepted 30 October 2020; published 24 November 2020)

Networks of coupled nonlinear oscillators allow for the formation of nontrivial partially synchronized spatiotemporal patterns, such as chimera states, in which there are coexisting coherent (synchronized) and incoherent (desynchronized) domains. These complementary domains form spontaneously, and it is impossible to predict where the synchronized group will be positioned within the network. Therefore, possible ways to control the spatial position of the coherent and incoherent groups forming the chimera states are of high current interest. In this work we investigate how to control chimera patterns in multiplex networks of FitzHugh-Nagumo neurons, and in particular we want to prove that it is possible to remotely control chimera states exploiting the multiplex structure. We introduce a pacemaker oscillator within the network: this is an oscillator that does not receive input from the rest of the network but is sending out information to its neighbors. The pacemakers can be positioned in one or both layers. Their presence breaks the spatial symmetry of the layer in which they are introduced and allows us to control the position of the incoherent domain. We demonstrate how the remote control is possible for both uni- and bidirectional coupling between the layers. Furthermore we show which are the limitations of our control mechanisms when it is generalized from single-layer to multilayer networks.

DOI: 10.1103/PhysRevE.102.052216

I. INTRODUCTION

Chimera states are intriguing phenomena of partial synchronization in oscillator networks. Kuramoto and Battogtokh first observed the coexistence of coherent and incoherent behavior in spatially symmetric oscillator networks in 2002 [1], and two years later these peculiar solutions were named chimera states by Abrams and Strogatz [2]. During the last two decades chimeras have become a popular topic in the nonlinear science community [3–18] and captured the interest of scientists from various disciplines, ranging from neuroscience, to chemistry, to engineering and many others. This widespread interest in the phenomenon led to the establishment of conceptual links between chimera states and real-world dynamics [7,19–35] and to the design of experiments which led to observation of chimera states in the laboratory [36–41].

Recently, a prominent line of research emerged which studies chimera states in multilayer networks [42–57]. Multilayer networks are important modeling tools for complex systems such as transportation networks, social interactions, and the brain [58,59]. Networks of neurons are one of the most promising applications of multilayer modeling [60]. Chimera states were observed in two- and three-layer networks of Hindmarsh-Rose neurons in Ref. [42]. In Refs. [43,44] Majhi and coauthors considered a two-layer network of Hindmarsh-Rose neurons and observed the emergence of chimera states via multiplexing when the neurons were uncoupled in one of the two layers. Synchronization between chimera states in multilayer networks was studied in recent research. In the study in Ref. [47] the authors detected generalized synchronization between chimera states in a two-layer network of phase oscillators. Subsequently, Ref. [50] was the first study of chimera states in a network with layers of different sizes. There the authors modeled a mean-field interlayer coupling and observed that the phases of the order parameters of the two layers synchronize [50]. In Ref. [49] it was shown that in a multiplex scheme with three layers formed by ring networks of FitzHugh-Nagumo oscillators, time delays can control relay synchronization between chimera states. The synchronization of chimera states in multiplex networks of phase oscillators with adaptive couplings within each layer was studied in Ref. [51].

It is known that in single-layer networks of finite size, chimera states show the following instabilities. First, chimeras are transients, and therefore they collapse to the stable synchronous state, although they can have a long lifetime [4,23]. Second, the complementary coherent and incoherent groups drift along the network [3], and therefore the spatial configuration of the chimera state varies in time. In small networks, these instabilities are particularly

*giuliaruzzene@gmail.com

pronounced. Furthermore, the initial position of the two groups is sensitively dependent on the initial conditions. The control of these instabilities of chimera states has been the subject of several studies which considered single-layer networks of various types of oscillators [61–68]. In contrast, control of chimera states in multilayer networks is still widely unexplored. In 2019 Omelchenko and coauthors showed that the so-called tweezers control mechanism introduced in Ref. [66] can also be used to control chimera states in multiplex networks of van der Pol oscillators [69]. In Ref. [56] the authors showed that it is possible to clone a chimera states from one layer to another of a multiplex network even when the coupling is active only for a short time. For a two-layer network of oscillatory FitzHugh-Nagumo units, a control strategy based on weak multiplexing was developed allowing one to induce or suppress chimera states [52].

It is therefore natural to ask whether other mechanisms to control chimera states may be effective in multilayer networks. Here we propose a method based on the interplay of a pacemaker oscillator [68] and the multiplex structure. Advantages of our method include its simple implementation and the fact that it does not require any feedback from the system. By acting only on the connectivity structure and leaving the oscillators unchanged, we are able to control the position of the incoherent region in one or both layers, with an efficiency that depends on the control configuration and the interlayer coupling strength.

The paper is organized as follows: first, we describe the model and integration methods (Sec. II A). Then we introduce measures for the control efficiency and for interlayer synchronization (Secs. II B and II C, respectively). We proceed with the results which are divided in two parts, obtained for unidirectional coupling (Sec. III A) and for bidirectional coupling (Sec. III B). We conclude with a brief discussion (Sec. IV).

II. METHODS

A. Model and integration

We study the dynamics of a two-layer network of FitzHugh-Nagumo oscillators. Each unit is characterized by two variables u and v. The layers are formed by N oscillators arranged in a ring topology. Following Ref. [6], inside each layer $l = 1, 2$, the oscillators are coupled nonlocally with range R and strength σ_l. The dynamics of the multiplex network is governed by the following set of differential equations for u_{lk}, v_{lk} and $k = 1, \ldots, N$ [52]:

$$
\begin{aligned}
\epsilon\frac{du_{1k}}{dt} &= u_{1k} - \frac{u_{1k}^3}{3} - v_{1k} + \frac{\sigma_1}{2R}\sum_{j=1}^{N} G_1(k,j)\{[b_{uu}(u_{1j}-u_{1k}) + b_{uv}(v_{1j}-v_{1k})]\} + \sigma_{2\to1}(u_{2k}-u_{1k}),\\
\frac{dv_{1k}}{dt} &= u_{1k} + a + \frac{\sigma_1}{2R}\sum_{j=1}^{N} G_1(k,j)\{[b_{vu}(u_{1j}-u_{1k}) + b_{vv}(v_{1j}-v_{1k})]\},\\
\epsilon\frac{du_{2k}}{dt} &= u_{2k} - \frac{u_{2k}^3}{3} - v_{2k} + \frac{\sigma_2}{2R}\sum_{j=1}^{N} G_2(k,j)\{[b_{uu}(u_{2j}-u_{2k}) + b_{uv}(v_{2j}-v_{2k})]\} + \sigma_{1\to2}(u_{1k}-u_{2k}),\\
\frac{dv_{2k}}{dt} &= u_{2k} + a + \frac{\sigma_2}{2R}\sum_{j=1}^{N} G_2(k,j)\{[b_{vu}(u_{2j}-u_{2k}) + b_{vv}(v_{2j}-v_{2k})]\}.
\end{aligned}
\tag{1}
$$

The bifurcation parameter a is set to 0.5 [6], so that each individual FitzHugh-Nagumo unit is in the oscillatory regime. The value of the time separation parameter ϵ is fixed at 0.05. The intralayer coupling scheme is constructed using a rotation matrix B (equal for both layers) and a coupling matrix G_l [6]:

$$
B = \begin{pmatrix} b_{uu} & b_{uv} \\ b_{vu} & b_{vv} \end{pmatrix} = \begin{pmatrix} \cos\phi & \sin\phi \\ -\sin\phi & \cos\phi \end{pmatrix}, \tag{2}
$$

$$
G_l(k,j) = \begin{cases} 1 & \text{if there is a link } j \to k \text{ in layer } l \\ 0 & \text{otherwise} \end{cases}, \tag{3}
$$

where $j, k = 1, \ldots, N$ and $l = 1, 2$. For nonlocal coupling with a rectangular coupling kernel of range R, the coupling matrix has the structure shown in Fig. 1(a) ($N = 50$, $R = 18$). It is known that for ϕ slightly smaller than $\frac{\pi}{2}$ the uncoupled layers show chimera states, so we set $\phi = \frac{\pi}{2} - 0.1$ throughout all simulations [6]. Regarding the interlayer coupling scheme, Eq. (1) models a bidirectional multiplex configuration where each oscillator's u_{1k} variable in layer 1 is coupled to the corresponding u_{2k} variable in layer 2, and vice versa [52]. The interlayer coupling strength is a scalar parameter $\sigma_{2\to1}$ from layer 2 to layer 1 and $\sigma_{1\to2}$ in the other direction. We also consider unidirectional coupling, i.e., a driver-response configuration which corresponds to $\sigma_{1\to2} > 0$ and $\sigma_{2\to1} = 0$. In Fig. 2 we give a schematic representation of all the network configurations used in this study, without and with a control mechanism.

We integrate the system using a fourth-order Runge-Kutta algorithm with a time step of 0.01 and we take an integration interval of 10^6 time steps. We then exclude transients from the measurements by taking an evaluation interval I in which the first 10^4 steps are discarded. Following Ref. [6], for each layer, initial conditions are taken to be uniformly distributed on a circle of radius 2.

B. Control impact

In this section we define some quantities that are used to analyze chimera state in a single-layer network. A geometric

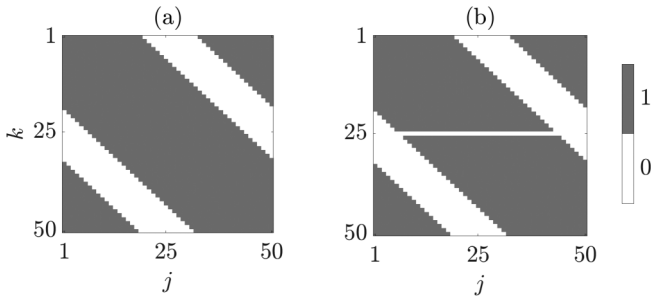

FIG. 1. Matrix representation of nonlocal coupling. (a) The connectivity matrix of a ring of nonlocally coupled oscillators. The network has $N = 50$ nodes and a rectangular coupling kernel with $R = 18$. (b) The modification of the connectivity matrix which corresponds to the presence of a pacemaker in position $p = 25$. All incoming connections of oscillator 25 are cut, which translates into the 25th row being set to 0.

phase is calculated for each oscillator [6]:

$$\theta_{lk} = \arctan \frac{v_{lk}}{u_{lk}} \quad \text{for } k = 1, \ldots, N.$$

This quantity is used to compute local order parameters and mean phase velocities, which serve as tools to display and detect chimeras:

$$Z_{lk} = \left| \frac{1}{2\delta + 1} \sum_{|m-k| \leqslant \delta} e^{i\theta_{lm}} \right|, \tag{4}$$

$$\omega_{lk} = \left\langle \frac{d\theta_{lk}}{dt} \right\rangle_I \quad \text{for } k = 1, \ldots, N \quad \text{and} \quad l = 1, 2, \tag{5}$$

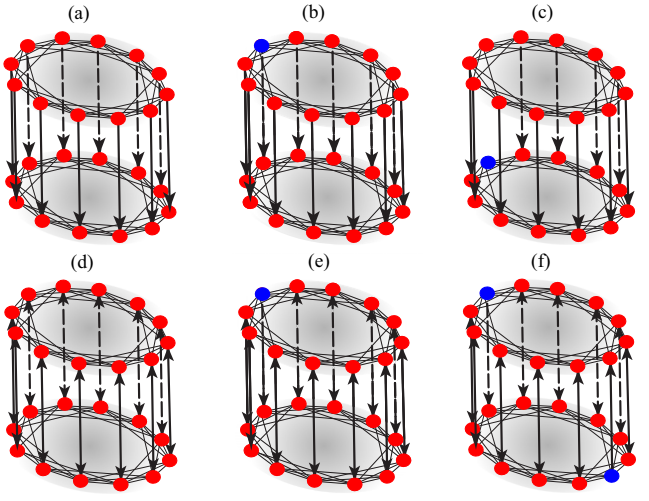

FIG. 2. Different combinations of multiplexing and control. All networks contain two rings of nonlocally coupled FitzHugh-Nagumo oscillators. The ring networks are highlighted in gray and the oscillator acting as a pacemaker in blue. The first row shows networks with unidirectional coupling, for which $\sigma_{2\to1} = 0$ and $\sigma_{1\to2>0}$. (a) No control. (b) Pacemaker in layer 1, position 25. (c) Pacemaker in layer 2, position 25. In the second row we show networks with bidirectional coupling between the layers and $\sigma_{1\to2} = \sigma_{2\to1}$. (d) No control. (e) Pacemaker in layer 1, position 25. (f) Pacemaker in layer 1, position 25 and in layer 2, position 50.

where i is the imaginary unit, δ determines the number of neighbors of one oscillator used to calculate its local order parameter, and $\langle\cdot\rangle_I$ is the time average over the evaluation interval I. As control mechanism, we use a pacemaker oscillator [68] in one or both layers. A pacemaker is an oscillator which is not receiving any input from the rest of the network but is sending output like all the others. Having a pacemaker in one of the layers corresponds to changing that layers' connectivity matrix G_l defined in Eq. (3). For example, a pacemaker in position $p_l = 25$ of layer l corresponds to setting to zero the 25th row of the matrix G_l defined in Eq. (3). This configuration is shown in Fig. 1(b) for $N = 50$ [70]. We want to study how the position of the chimera's incoherent group in the two layers of the network in Eq. (1) is affected by the interplay of multiplexing and control with a pacemaker. To do so, following the algorithm in Appendix B of Ref. [68], we calculate the position $c_l(t)$ of the center of the chimera's incoherent group. The center position $c_l(t)$ takes integer and half-integer values c in the interval $[0.5, N]$. We then define a binary function χ_l that codifies the evolution of the center position in space and time for each layer:

$$\chi_l(c,t) = \begin{cases} 1 & \text{if } c = c_l(t) \\ 0 & \text{otherwise} \end{cases}. \tag{6}$$

We define $\gamma_l(c) = \langle \chi_l(c,t) \rangle_I$, which determines the fraction of times for which the center of the incoherent group is in any possible position c. We then define the control impact $\Gamma_l(p_l, \Delta)$ for a pacemaker in position p_l as

$$\Gamma_l(p_l, \Delta) = \sum_{c=p_l-\Delta}^{p_l+\Delta} \gamma_l(c). \tag{7}$$

This control impact measures how many times the center of the chimera's incoherent group lies in a neighborhood of width $2\Delta + 1$ of the pacemaker position p_l during the interval I. In Fig. 3(a) we show a chimera state in a single-layer network of FitzHugh-Nagumo oscillators without any control. In this case the corresponding distribution $\gamma(c)$ is almost flat [Fig. 3(b)]. If we introduce a pacemaker in position $p = 25$ and we solve Eq. (1) starting from the same intial condition, then we obtain the chimera state in Fig. 3(c), which has the incoherent group centered around the pacemaker position. Now $\gamma(c)$ has a peak around position 25 [Fig. 3(d)]. The area highlighted in green in Figs. 3(b) and 3(d) corresponds to the control impact Γ_l. It follows from the definition (7) that the control impact takes values between 0 and 1. In an uncontrolled network, there is no preferred position for the center of the incoherent group. Therefore, when the evaluation interval I becomes arbitrarily large, the expected value of Γ_l is $\frac{4\Delta+1}{2N}$. This means that the center of the chimera's incoherent group is equally likely to occupy all positions $c \in [0.5, N]$ while it drifts along the network. However, here we show results for finite simulation times, therefore we cannot see a constant value of Γ even when there is no control. This is because there is no preferred initial position for the center of the incoherent group and the drifting is not fast enough to allow the center of the incoherent group to spend the same amount of time in all available positions.

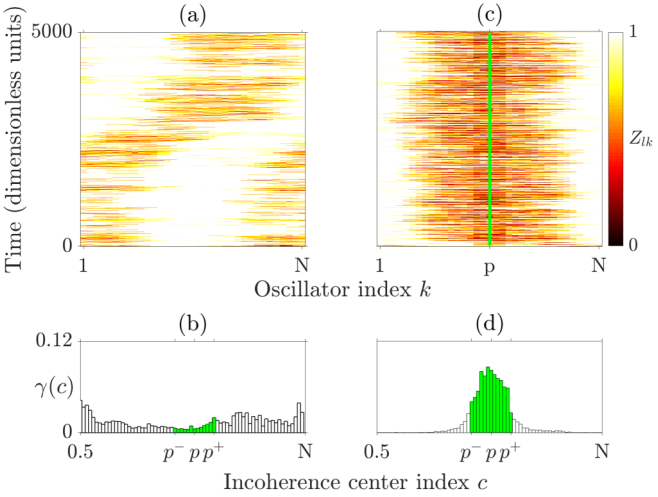

FIG. 3. A pacemaker controls the position of a chimera state in a single-layer network on FitzHugh-Nagumo oscillators. (a), (c) Space-time plots of Z_{lk} without control (left column) and with a pacemaker in position $p = 25$ (right column). (b), (d) The distribution γ of the position of the center of incoherence. The green area corresponds to the control impact $\Gamma(25, 5)$ where $p = 25$ and $\Delta = 5$. In panels (b) and (d) we define $p^- = p - \Delta$ and $p^+ = p + \Delta$. Network parameters: $N = 50, R = 18, \sigma = 0.2, \phi = \pi/2 - 0.1, a = 0.5, \varepsilon = 0.05$.

C. Quantification of synchronization

To assess the interplay between chimera states across the two layers we here introduce two quantities that measure the alignment of the incoherent groups of the chimera states and the interlayer synchronization of the two dynamics. First, we measure the degree to which the chimera states in the two layers align their position. To do this we calculate the difference between the position of the centers of the incoherent groups c_1, c_2 in the two layers on a circumference of length N:

$$D_{12} = \langle \min\{|c_1(t) - c_2(t)|, N - |c_1(t) - c_2(t)|\}\rangle_I. \quad (8)$$

A value of $D_{12} = 0$ denotes alignment of the incoherent groups, while if $D_{12} = N/2$ the center of the two incoherent groups are in antipodal positions. To quantify synchronization between the two layers we use the measures introduced in Ref. [49]. For $k = 1, \ldots, N$, the local interlayer synchronization error is defined as

$$E_{12}(k) = \langle \|x_{1k}(t) - x_{2k}(t)\|\rangle_I, \quad (9)$$

where $x_{lk} = \begin{bmatrix} u_{lk} \\ v_{lk} \end{bmatrix}$ for $l = 1, 2$. By taking also the spatial average in Eq. (9), one obtains the global interlayer synchronization error [49]:

$$E_{12} = \frac{1}{N}\sum_{k=1}^{N} E_{12}(k). \quad (10)$$

III. RESULTS

In this section we present results about control of chimera states obtained for unidirectional coupling and bidirectional coupling between the layers. The results are shown in Figs. 4 through 9, and detailed information about the parameters used

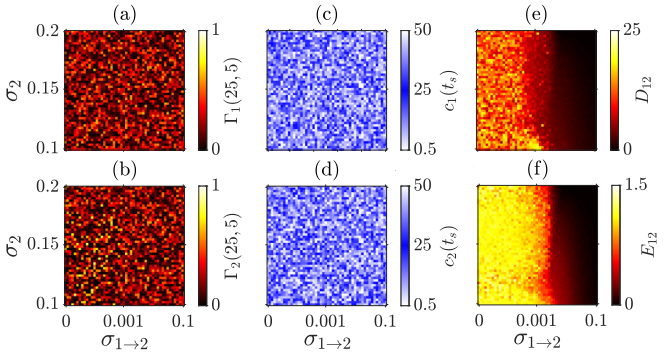

FIG. 4. Effect of unidirectional coupling on chimera states in a two-layer network of FitzHugh-Nagumo oscillators in the parameter space of the interlayer coupling $\sigma_{1\to2}$ and intralayer coupling σ_2 without pacemaker [see Fig. 2(a)]. The interlayer coupling $\sigma_{1\to2}$ varies from 10^{-5} to 10^{-1} and is sampled on a logarithmic scale, while $\sigma_{2\to1}$ is kept equal to 0. We then added a column of results for $\sigma_{1\to2} = 0$, corresponding to isolated layers. The intralayer coupling σ_2 varies linearly from 0.1 to 0.2. Other parameters are $N = 50$, $R = 18, \sigma_1 = 0.2, \phi = \pi/2 - 0.1, a = 0.5, \epsilon = 0.05$. Panels (a) and (b) show control impact values $\Gamma_1(25, 5)$ and $\Gamma_2(25, 5)$, while panels (c) and (d) are snapshots of the position $c_l(t_s)$ of the center of incoherence in layer $l = 1, 2$, respectively, at time $t_s = 500\,000$ time steps. (e) and (f) Synchronization measures: (e) alignment D_{12} and (f) global synchronization error E_{12}.

in the simulations is given in the caption of Fig. 4. The results are presented with the same configuration for different combinations of multiplex coupling schemes and positions of the pacemaker. The figures are composed of two rows of three panels each, the first two columns show single-layer quantities, while the last one shows multilayer quantities. In Figs. 4, 5, 6, 7, 8, 9 panels (a), (b), (c), and (d) show the control impact Γ values and a snapshot of the LCG center position c for layer 1 and layer 2, respectively. For Γ, yellow means that the positions of chimera states are controlled. In this case the position of the center of the LCG takes values that are close to the pacemaker position. If there is no control, we observe a speckled pattern for c. In panel (e) we show the alignment of the LCG centers D_{12} and in panel (f) the global synchronization error E_{12}. We vary the interlayer coupling strength $\sigma_{1\to2}$ between a minimum of 0 (corresponding to isolated layers) and a maximum of 0.05. Furthermore, we keep $\sigma_1 = 0.2$, and we vary σ_2 in the interval [0.1,0.2].

A. Unidirectional coupling

First, we consider the case of unidirectional interlayer coupling from layer 1 to layer 2. We study three possible configurations: without any control, with a pacemaker in layer 1 in position $p_1 = 25$, and finally with a pacemaker in layer 2 in position $p_2 = 25$ while layer 1 is uncontrolled.

Figures 4(a) and 4(b) confirm that in the absence of a control mechanism there cannot be any preferred position for the center of the incoherent group. This is reflected in values of $\Gamma_1(25, 5)$ and $\Gamma_2(25, 5)$ that are close to the expected value of $\frac{4\Delta_l+1}{2N}$. This means that in each realization the drifting causes the chimera's center to occupy all positions almost uniformly. This is confirmed by the snapshot of the centers

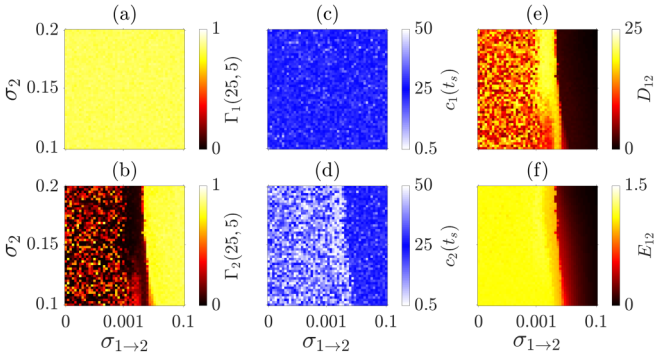

FIG. 5. With unidirectional coupling between the layers, it is possible to remotely control chimera states in layer 2 using a pacemaker only in layer 1. Same network configuration and parameters as in Fig. 4, but here there is a pacemaker in layer 1 in position $p_1 = 25$ [see Fig. 2(b)].

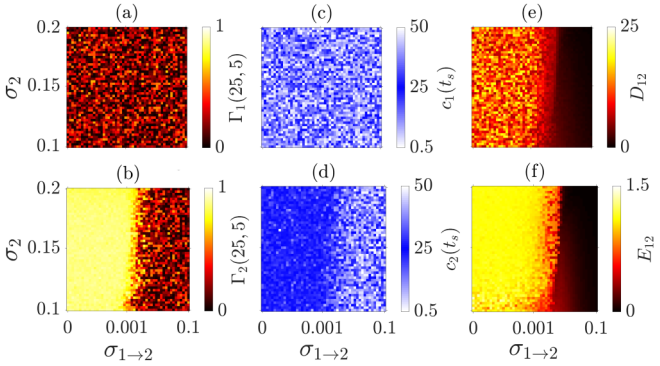

FIG. 6. The driving effect becomes stronger than the pacemaker effect for increasing interlayer coupling. Same network configuration and parameters as in Fig. 4, but here there is a pacemaker in layer 2 in position $p_2 = 25$ [see Fig. 2(c)].

of incoherence shown in Figs. 4(c) and 4(d). At a certain moment in time, the center of incoherence is in different positions in different realizations. The incoherent groups of the chimera states align for strong interlayer coupling [dark area in Fig. 4(e)] and, in general, the two layers synchronize their dynamics, as is shown in Fig. 4(f), where the global synchronization error E_{12} reaches values close to zero.

The scenario described so far in the uncontrolled case is quite intuitive, while it is less obvious what happens when there is also a pacemaker present in the network. The results for the second configuration, obtained for a network with a pacemaker in position $p_1 = 25$ of the driving layer (layer 1), are shown in Fig. 5. Because of the unidirectional coupling, layer 1 is not receiving any input from layer 2, therefore it behaves as an isolated ring network. The almost constant value of $\Gamma_1(25, 5)$ close to 1 shows that the pacemaker can control the position of a chimera state [Fig. 5(a)] in an isolated layer of FitzHugh-Nagumo oscillators. These results generalize our observations for phase oscillators [68] to FitzHugh-Nagumo oscillators. The question now is whether the pacemaker in layer 1 can remotely control the position of the chimera state in layer 2 via the coupling. When the two chimeras in the two layers are aligned [see Figs. 5(e) and 5(f)], we see that the answer is affirmative [yellow region in Fig. 5(b)]. It is worth noticing that before the control becomes effective in layer 2 there is an intermediate region of parameters in which we observe that the center of the incoherent group in layer 2 tends to be diametrically opposed to the pacemaker position [yellow region in Fig. 5(e)]. Therefore the distance between the centers of the two low coherence groups reaches its maximum. The pacemaker has a repulsive action on the center of incoherence in layer 2 before the remote control starts to be effective.

Another interesting question is which one is stronger, the pacemaker or the driving? To address this problem, we move to the third configuration. In this case we still have unidirectional coupling from layer 1 to layer 2 and a pacemaker only in position $p_2 = 25$ of layer 2. As a consequence, there is no preferred position for the chimera states in layer 1, as we can see from the values of $\Gamma_1(25, 5)$ in Fig. 6(a). In fact, Fig. 6(a) is qualitatively similar to Fig. 4(a), since slight differences are due only to different realizations of the network in layer 1. As the chimera states align for high values of the interlayer coupling $\sigma_{1\to2}$ [Figs. 6(b) and 6(e)], the driving effect of layer 1 eventually wins over the controlling effect of the pacemaker in layer 2 [Fig. 6(b)]. Nevertheless, it is interesting that there is a wide region of parameter space in which it is possible to control the position of the chimera in layer 2 despite the driving by layer 1.

B. Bidirectional coupling

We now consider bidirectional interlayer coupling and three possible configurations: without any control, with a pacemaker in layer 1 in position $p_1 = 25$, and finally with two conflicting pacemakers, one in layer 1 in position $p_1 = 25$ and one in layer 2 in position $p_2 = 50$. We vary the parameter σ_2 like in the unidirectional case and the parameter $\sigma_{1\leftrightarrow2}$ like $\sigma_{1\to2}$ in the unidirectional case.

In the first configuration (Fig. 7), we observe a similarity with the results obtained in the case of unidirectional coupling (Fig. 4). In this case, again there cannot be any preferred position for the chimera states in the two layers [Figs. 7(a) and 7(b)]. This is reflected also in the snapshots of the center position $c_{1,2}(t_s)$ in Figs. 7(c) and 7(d). The incoherent groups become aligned through a monotonic process [Fig. 7(e)], and

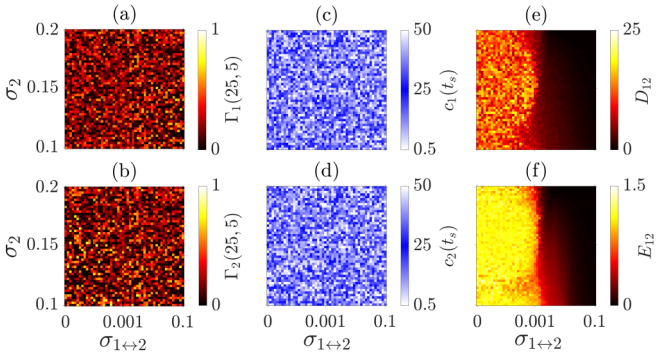

FIG. 7. Results for a duplex network of FitzHugh-Nagumo oscillators with bidirectional coupling. All network parameters are the same as in Fig. 4, except we have $\sigma_{2\to1} = \sigma_{1\to2} \equiv \sigma_{1\leftrightarrow2}$ [see Fig. 2(d)].

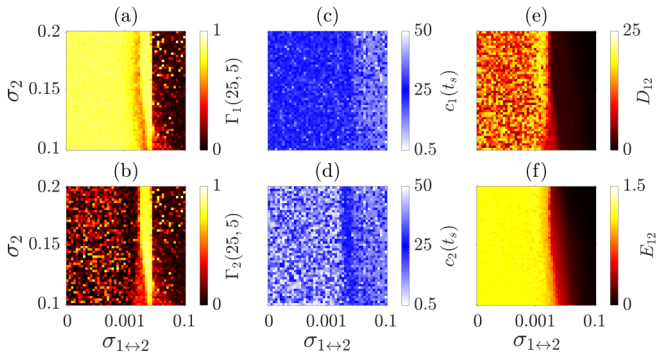

FIG. 8. Bidirectional coupling makes remote control via a pacemaker more difficult. Same network configuration and parameters as in Fig. 7, but here a pacemaker is present in layer 1, position $p_1 = 25$ [see Fig. 2(e)].

in the same way the dynamics of the two layers become synchronized for increasing interlayer coupling [Fig. 7(f)].

The second configuration, in which a pacemaker is present in layer 1 at position $p_1 = 25$, leads to results that are different from the unidirectional case. In Fig. 8(a) we see that the pacemaker is able to control the chimera's position in layer 1 only up to a certain value of interlayer coupling $\sigma_{1\leftrightarrow 2}$ (yellow region). Above this value, the coupling between the layers takes over and the chimera states are aligned [Fig. 8(e)] but still do not have a preferred position. The main difference with the unidirectional case is that the remote control of the chimera state in layer 2 via the pacemaker in layer 1 and the coupling is possible only in a small region of the parameter space [yellow stripe in Fig. 8(b)].

In the third and last configuration we have conflicting pacemakers trying to control the chimera states in the two layers, one in layer 1 in position $p_1 = 25$ and one in layer 2 in position $p_2 = 50$. In this case we see that the control works in both layers in a certain region of the parameter space, corresponding to the yellow areas in Figs. 9(a) and 9(b). Note that there is another small region for which the control in layer 1 continues to work. A similar effect, even more pronounced, is observed with a single pacemaker in layer 1 [Fig. 8(a)] and

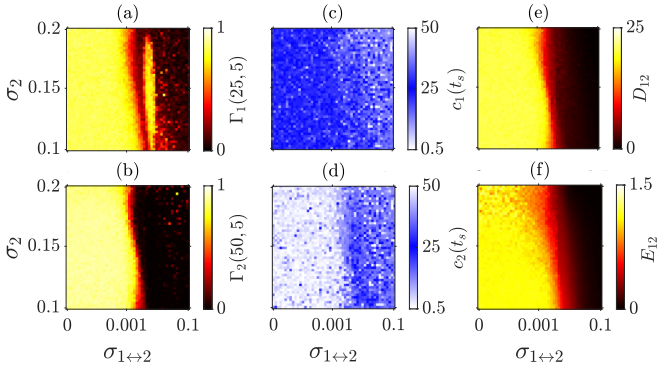

FIG. 9. Conflicting pacemakers and bidirectional coupling cause the chimera states to compromise on their position. Same network configuration and parameters as in Fig. 7, but here in each layer there is a pacemaker, in position $p_1 = 25$ and $p_2 = 50$ [see Fig. 2(f)].

is correlated with antipodal alignment in Fig. 8(e). An analogous effect can also be observed in the transition to remote control with unidirectional coupling and a pacemaker in layer 1 [Fig. 5(e)]. For stronger interlayer coupling, the control effect ceases to prevail, but the chimeras become aligned, as is to be expected [see Fig. 9(e)]. Interestingly, the two centers are aligned, but their positions do not coincide with either of the pacemakers' positions, as we can deduce from the low values of both coupling impact measures $\Gamma_1(25, 5)$ and $\Gamma_2(50, 5)$ [rightmost part of Figs. 9(a) and 9(b)]. Looking at the center snapshots in Figs. 9(c) and 9(d), we see that the center is positioned close to 12.5 or 37.5, which are halfway from the pacemakers' positions. It is worth noticing that the synchronization region in Fig. 9(f) becomes smaller when two or more pacemakers are present in the network.

IV. DISCUSSION

To summarize, in a duplex network with a driver-response configuration given by unidirectional coupling between the layers, we observe a nontrivial interplay between pacemaker control of chimera states and interlayer synchronization that can be used to construct networks in which chimera states are present in both layers and in certain positions. Furthermore, the possibility of controlling remotely the chimera states in layer 2 via a pacemaker in layer 1 is important for scenarios in which there is limited access to some parts of the network. A bidirectional coupling scheme makes the remote control of layer 2 via a pacemaker in layer 1 more difficult. When there are two conflicting pacemakers, for low values of interlayer coupling, both pacemakers attract the incoherent groups to their respective positions. As the coupling becomes stronger, the incoherent groups of the chimeras in the two layers align in a position that is halfway between the two pacemakers.

Interestingly, in previous studies, pacemakers were generally used to promote full synchronization [71,72]. It is remarkable that the same tool can be used for a completely different purpose when it is combined with the nonlocal coupling configuration. In general, we find that it is a nontrivial problem to transfer control methods for chimera states from single-layer networks to multilayer networks, given the many possible configurations in which this can be done. We show that there are ample regions of the parameter space in which the control mechanism developed in Ref. [68] allows one to to control chimeras in one or both layers. The present study generalizes the finding of Ref. [68] in two directions: we go from phase to FitzHugh-Nagumo oscillators and from single-layer to two-layer multiplex networks. It will be interesting in the future to further investigate the counterintuitive effect in Fig. 5. There the control becomes effective through a nonmonotonic process. We observe a resistance of layer 2 to being remotely controlled by layer 1, in the sense that the center of incoherence in layer 2 positions itself as far as possible from the pacemaker position before the control becomes effective.

Our control mechanism has several features which make it appealing to applications of experimental settings. Among these are its simple implementation, and the fact that it does not require one to use feedback from the system nor

to modify the dynamics of the individual oscillators. The model that we use is quite simple, but it serves our general purpose of studying ways to control partial synchronization patterns in scenarios that can be associated with brain dynamics [29,30,34,73]. Therefore, our results may provide a base to develop methods to control chimera states in experiments and real-world scenarios.

ACKNOWLEDGMENTS

This project was supported by the Spanish Ministry of Economy and Competitiveness, Grant No. FIS2014-54177-R (G.R. and R.G.A.). We acknowledge support from the Deutsche Forschungsgemeinschaft (DFG) in the framework of the SFB 910, Projektnummer 163436311 (I.O., G.R., J.S., E.S. and A.Z.).

[1] Y. Kuramoto and D. Battogtokh, Coexistence of coherence and incoherence in nonlocally coupled phase oscillators, Nonlin. Phenom. Complex Syst. **4**, 380 (2002).

[2] D. M. Abrams and S. H. Strogatz, Chimera States for Coupled Oscillators, Phys. Rev. Lett. **93**, 174102 (2004).

[3] O. E. Omel'chenko, M. Wolfrum, and Y. L. Maistrenko, Chimera states as chaotic spatiotemporal patterns, Phys. Rev. E **81**, 065201(R) (2010).

[4] M. Wolfrum and O. E. Omel'chenko, Chimera states are chaotic transients, Phys. Rev. E **84**, 015201(R) (2011).

[5] J. Hizanidis, V. G. Kanas, A. Bezerianos, and T. Bountis, Chimera states in networks of nonlocally coupled Hindmarsh-Rose neuron models, Int. J. Bifurcation Chaos **24**, 1450030 (2014).

[6] I. Omelchenko, O. E. Omel'chenko, P. Hövel, and E. Schöll, When Nonlocal Coupling Between Oscillators Becomes Stronger: Patched Synchrony or Multichimera States, Phys. Rev. Lett. **110**, 224101 (2013).

[7] L. Schmidt, K. Schönleber, K. Krischer, and V. García-Morales, Coexistence of synchrony and incoherence in oscillatory media under nonlinear global coupling, Chaos **24**, 013102 (2014).

[8] Y. Suda and K. Okuda, Persistent chimera states in nonlocally coupled phase oscillators, Phys. Rev. E **92**, 060901(R) (2015).

[9] B. K. Bera and D. Ghosh, Chimera states in purely local delay-coupled oscillators, Phys. Rev. E **93**, 052223 (2016).

[10] A. Zakharova, M. Kapeller, and E. Schöll, Chimera Death: Symmetry Breaking in Dynamical Networks, Phys. Rev. Lett. **112**, 154101 (2014).

[11] C. Bick, M. Sebek, and I. Z. Kiss, Robust Weak Chimeras in Oscillator Networks with Delayed Linear and Quadratic Interactions, Phys. Rev. Lett. **119**, 168301 (2017).

[12] S. A. Bogomolov, A. V. Slepnev, G. I. Strelkova, E. Schöll, and V. S. Anishchenko, Mechanisms of appearance of amplitude and phase chimera states in ensembles of nonlocally coupled chaotic systems, Commun. Nonlin. Sci. Numer. Simul. **43**, 25 (2017).

[13] I. Omelchenko, A. Provata, J. Hizanidis, E. Schöll, and P. Hövel, Robustness of chimera states for coupled FitzHugh-Nagumo oscillators, Phys. Rev. E **91**, 022917 (2015).

[14] O. E. Omel'chenko, The mathematics behind chimera states, Nonlinearity **31**, R121 (2018).

[15] O. E. Omel'chenko and E. Knobloch, Chimerapedia: Coherence-incoherence patterns in one, two and three dimensions, New J. Phys. **21**, 093034 (2019).

[16] J. Sawicki, I. Omelchenko, A. Zakharova, and E. Schöll, Delay-induced chimeras in neural networks with fractal topology, Eur. Phys. J. B **92**, 54 (2019).

[17] A. Zakharova, *Chimera Patterns in Networks: Interplay between Dynamics, Structure, Noise and Delay*, Understanding Complex Systems (Springer, Berlin, 2020).

[18] E. Schöll, A. Zakharova, and R. G. Andrzejak, Editorial on the research topic: Chimera states in complex networks, Front. Appl. Math. Stat. **5**, 62 (2019).

[19] L. Larger, B. Penkovsky, and Y. Maistrenko, Virtual Chimera States for Delayed-Feedback Systems, Phys. Rev. Lett. **111**, 054103 (2013).

[20] J. C. González-Avella, M. G. Cosenza, and M. San Miguel, Localized coherence in two interacting populations of social agents, Physica A **399**, 24 (2014).

[21] L. V. Gambuzza, A. Buscarino, S. Chessari, L. Fortuna, R. Meucci, and M. Frasca, Experimental investigation of chimera states with quiescent and synchronous domains in coupled electronic oscillators, Phys. Rev. E **90**, 032905 (2014).

[22] V. M. Bastidas, I. Omelchenko, A. Zakharova, E. Schöll, and T. Brandes, Quantum signatures of chimera states, Phys. Rev. E **92**, 062924 (2015).

[23] R. G. Andrzejak, C. Rummel, F. Mormann, and K. Schindler, All together now: Analogies between chimera state collapses and epileptic seizures, Sci. Rep. **6**, 23000 (2016).

[24] T. Banerjee, P. S. Dutta, A. Zakharova, and E. Schöll, Chimera patterns induced by distance-dependent power-law coupling in ecological networks, Phys. Rev. E **94**, 032206 (2016).

[25] S. A. M. Loos, J. C. Claussen, E. Schöll, and A. Zakharova, Chimera patterns under the impact of noise, Phys. Rev. E **93**, 012209 (2016).

[26] N. E. Kouvaris, R. J. Requejo, J. Hizanidis, and A. Díaz-Guilera, Chimera states in a network-organized public goods game with destructive agents, Chaos **26**, 123108 (2016).

[27] J. Hizanidis, N. Lazarides, and G. P. Tsironis, Robust chimera states in squid metamaterials with local interactions, Phys. Rev. E **94**, 032219 (2016).

[28] J. Hizanidis, N. E. Kouvaris, G. Zamora-López, A. Díaz-Guilera, and C. G. Antonopoulos, Chimera-like states in modular neural networks, Sci. Rep. **6**, 19845 (2016).

[29] T. Chouzouris, I. Omelchenko, A. Zakharova, J. Hlinka, P. Jiruska, and E. Schöll, Chimera states in brain networks: Empirical neural vs. modular fractal connectivity, Chaos **28**, 045112 (2018).

[30] K. Bansal, J. O. Garcia, S. H. Tompson, T. Verstynen, J. M. Vettel, and S. F. Muldoon, Cognitive chimera states in human brain networks, Sci. Adv. **5**, eeau8536 (2019).

[31] L. Ramlow, J. Sawicki, A. Zakharova, J. Hlinka, J. C. Claussen, and E. Schöll, Partial synchronization in empirical brain networks as a model for uniemispheric sleep, Europhys. Lett. **126**, 50007 (2019).

[32] L. Kang, C. Tian, S. Huo, and Z. Liu, A two-layered brain network model and its chimera state, Sci. Rep. **9**, 14389 (2019).
[33] E. Rybalova, A. Bukh, G. Strelkova, and V. Anischenko, Spiral and target-wave chimeras in a 2D lattice of map-based neuron models, Chaos **29**, 101104 (2019).
[34] A. Pournaki, L. Merfort, J. Ruiz, N. E. Kouvaris, P. Hövel, and J. Hizanidis, Synchronization patterns in modular neuronal networks: A case study of *C. elegans*, Front. Appl. Math. Stat. **5**, 52 (2019).
[35] S. Kundu, S. Majhi, and D. Ghosh, From asynchronous to synchronous chimeras in ecological multiplex networks, Eur. Phys. J.: Spec. Top. **228**, 2429 (2019).
[36] A. M. Hagerstrom, T. E. Murphy, R. Roy, P. Hoevel, I. Omelchenko, and E. Schöll, Experimental observation of chimeras in coupled-map lattices, Nat. Phys. **8**, 658 (2012).
[37] M. R. Tinsley, S. Nkomo, and K. Showalter, Chimera and phase-cluster states in populations of coupled chemical oscillators, Nat. Phys. **8**, 662 (2012).
[38] E. A. Martens, S. Thutupalli, A. Fourrière, and O. Hallatschek, Chimera states in mechanical oscillator networks, Proc. Natl. Acad. Sci. USA **110**, 10563 (2013).
[39] M. Wickramasinghe and I. Z. Kiss, Spatially organized dynamical states in chemical oscillator networks: Synchronization, dynamical differentiation, and chimera patterns, PLoS ONE **8**, e80586 (2013).
[40] J. D. Hart, K. Bansal, T. E. Murphy, and R. Roy, Experimental observation of chimera and cluster states in a minimal globally coupled network, Chaos **26**, 094801 (2016).
[41] J. F. Totz, J. Rode, M. R. Tinsley, K. Showalter, and H. Engel, Spiral wave chimera states in large populations of coupled chemical oscillators, Nat. Phys. **14**, 282 (2018).
[42] V. A. Maksimenko, V. V. Makarov, B. K. Bera, D. Ghosh, S. K. Dana, M. V. Goremyko, N. S. Frolov, A. A. Koronovskii, and A. E. Hramov, Excitation and suppression of chimera states by multiplexing, Phys. Rev. E **94**, 052205 (2016).
[43] S. Majhi, M. Perc, and D. Ghosh, Chimera states in uncoupled neurons induced by a multilayer structure, Sci. Rep. **6**, 39033 (2016).
[44] S. Majhi, M. Perc, and D. Ghosh, Chimera states in a multilayer network of coupled and uncoupled neurons, Chaos **27**, 073109 (2017).
[45] A. Bukh, E. Rybalova, N. Semenova, G. Strelkova, and V. Anishchenko, New type of chimera and mutual synchronization of spatiotemporal structures in two coupled ensembles of nonlocally interacting chaotic maps, Chaos **27**, 111102 (2017).
[46] M. Goremyko, V. Maksimenko, V. Makarov, D. Ghosh, B. Bera, S. Dana, and A. Hamrow, Interaction of Chimera States in a Multilayereed Network of Nonlocally Coupled Oscillators, Tech. Phys. Lett. **43**, 712 (2017).
[47] R. G. Andrzejak, G. Ruzzene, and I. Malvestio, Generalized synchronization between chimera states, Chaos **27**, 053114 (2017).
[48] S. Ghosh, A. Zakharova, and S. Jalan, Non-identical multiplexing promotes chimera states, Chaos Solitons Fractals **106**, 56 (2018).
[49] J. Sawicki, I. Omelchenko, A. Zakharova, and E. Schöll, Delay controls chimera relay synchronization in multiplex networks, Phys. Rev. E **98**, 062224 (2018).
[50] R. G. Andrzejak, G. Ruzzene, I. Malvestio, K. Schindler, E. Schöll, and A. Zakharova, Mean field phase synchronization between chimera states, Chaos **28**, 091101 (2018).
[51] D. V. Kasatkin and V. I. Nekorkin, Synchronization of chimera states in a multiplex system of phase oscillators with adaptive couplings, Chaos **28**, 093115 (2018).
[52] M. Mikhaylenko, L. Ramlow, S. Jalan, and A. Zakharova, Weak multiplexing in neural networks: Switching between chimera and solitary states, Chaos **29**, 023122 (2019).
[53] E. Rybalova, T. Vadisova, G. Strelkova, V. Anishchenko, and A. S. Zakharova, Forced synchronization of a multilayer heterogeneous network of chaotic maps in the chimera state mode, Chaos **29**, 033134 (2019).
[54] M. Winkler, J. Sawicki, I. Omelchenko, A. Zakharova, V. Anishchenko, and E. Schöll, Relay synchronization in multiplex networks of discrete maps, Europhys. Lett. **126**, 50004 (2019).
[55] D. Nikitin, I. Omelchenko, A. Zakharova, M. Avetyan, A. L. Fradkov, and E. Schöll, Complex partial synchronization patterns in networks of delayed-coupled neurons, Philos. Trans. R. Soc. London A **377**, 20180128 (2019).
[56] A. Dmitrichev, D. Shchapin, and V. Nekorkin, Cloning of chimera states in a large short-term coupled multiplex network of relaxation oscillators, Front. Appl. Math. Stat. **5**, 9 (2019).
[57] F. Drauschke, J. Sawicki, R. Berner, I. Omelchenko, and E. Schöll, Effect of topology upon relay synchronization in triplex neuronal networks, Chaos **30**, 051104 (2020).
[58] S. Boccaletti, G. Bianconi, R. Criado, C. del Genio, J. Gmez-Gardees, M. Romance, I. Sendia-Nadal, Z. Wang, and M. Zanin, The structure and dynamics of multilayer networks, Phys. Rep. **544**, 1 (2014).
[59] M. De Domenico, Multilayer modeling and analysis of human brain networks, GigaScience **6**, 1 (2017).
[60] S. Majhi, B. Bera, D. Ghosh, and M. Perc, Chimera states in neuronal networks: A review, Phys. Life Rev. **28**, 101 (2019).
[61] J. Sieber, O. E. Omel'chenko, and M. Wolfrum, Controlling Unstable Chaos: Stabilizing Chimera States by Feedback, Phys. Rev. Lett. **112**, 054102 (2014).
[62] C. Bick and E. A. Martens, Controlling chimeras, New J. Phys. **17**, 33030 (2015).
[63] L. V. Gambuzza and M. Frasca, Pinning control of chimera states, Phys. Rev. E **94**, 022306 (2016).
[64] T. Isele, J. Hizanidis, A. Provata, and P. Hövel, Controlling chimera states: The influence of excitable units, Phys. Rev. E **93**, 022217 (2016).
[65] A. Gjurchinovski, E. Schöll, and A. Zakharova, Control of amplitude chimeras by time delay in oscillator networks, Phys. Rev. E **95**, 042218 (2017).
[66] I. Omelchenko, O. E. Omel'chenko, A. Zakharova, M. Wolfrum, and E. Schöll, Tweezers for Chimeras in Small Networks, Phys. Rev. Lett. **116**, 114101 (2016).
[67] I. Omelchenko, O. E. Omel'chenko, A. Zakharova, and E. Schöll, Optimal design of tweezer control for chimera states, Phys. Rev. E **97**, 012216 (2018).
[68] G. Ruzzene, I. Omelchenko, E. Schöll, A. Zakharova, and R. G. Andrzejak, Controlling chimera states via minimal coupling modification, Chaos **29**, 051103 (2019).
[69] I. Omelchenko, T. Hülser, A. Zakharova, and E. Schöll, Control of chimera states in multilayer networks, Front. Appl. Math. Stat. **4**, 67 (2019).

[70] When we have a pacemaker in position p_l of layer l we also multiply by 0 the interlayer coupling term $\sigma_{1\to 2}(u_{1p_l} - u_{2p_l})$ and/or $\sigma_{2\to 1}(u_{2p_l} - u_{1p_l})$, depending if the pacemaker is in layer 1, in layer 2 or in both layers.

[71] H. Kori and A. S. Mikhailov, Entrainment of Randomly Coupled Oscillator Networks by a Pacemaker, Phys. Rev. Lett. **93**, 254101 (2004).

[72] F. Radicchi and H. Meyer-Ortmanns, Entrainment of coupled oscillators on regular networks by pacemakers, Phys. Rev. E **73**, 036218 (2006).

[73] M. Gerster, R. Berner, J. Sawicki, A. Zakharova, A. Skoch, J. Hlinka, K. Lenhertz, and E. Schöll, FitzHugh-Nagumo oscillators on complex networks mimic epileptic-seizure-related synchronization phenomena, arXiv:2007.05497.